A Photoactive Semisynthetic Metalloenzyme Exhibits Complete Selectivity for CO_2 Reduction in Water

Camille R. Schneider, Anastasia C. Manesis, Michael J. Stevenson, and Hannah S. Shafaat

Electronic Supporting Information

Table of Contents

Materials and Methods
All materials and reagents were used as received unless specifically noted.

Sequencing data

For all Az mutants (sequences below), standard heterologous expression techniques were used. The *Pseudomonas aeruginosa (Pae*) wild-type (WT) Az gene was encoded into a pUC18 plasmid, which was generously donated by Professor Judy Kim (UCSD). The Az mutants studied were created using the following mutagenic primers (Sigma Aldrich):

5'-GACGGTATGGCTTGCGGTCTGGATAAAG-3'	(S66C forward)
5'-CTTTATCCAGACCGCAAGCCATACCGTC-3'	(S66C reverse)
5'-GCCGGATGACTGCCGAGTTATCGCC-3'	(S78C forward)
5'-GGCGATAACTCGGCAGTCATCCGGC-3'	(S78C reverse)
5'-CGTTACTTTCGACGTTTGCAAGCTTAAAGAAGG-3'	(S100C forward)
5'-CCTTCTTTAAGCTTGCAAACGTCGAAAGTAACG-3'	(S100C reverse)

S66C Az DNA sequence:

GCT GAA TGC TCC GTT GAT ATC CAG GGT AAT GAT CAG
ATG CAG TTC AAC ACC AAC GCC ATC ACC GTC GAC AAG
AGC TGC AAG CAG TTC ACT GTT AAC CTG TCT CAC CCA
GGT AAC CTG CCG AAG AAC GTT ATG GGT CAC AAC TGG
GTT CTG TCC ACC GCG GCT GAC ATG CAA GGC GTT GTC
ACT GAC GGT ATG GCT **TGC** GGT CTG GAT AAA GAC TAC
CTG AAG CCG GAT GAC TCT CGA GTT ATC GCC CAC ACC
AAG CTG ATC GGA TCC GGT GAA AAA GAC TCC GTT ACT
TTC GAC GTT TCC AAG CTT AAA GAA GGT GAA CAG TAC
ATG TTC TTC TGC ACT TTC CCG GGT CAC TCC GCA CTG
ATG AAA GGT ACC CTG ACT CTG AAA TAG

S66C Az amino acid sequence:

AECSVDIQGNDQMQFNTNAITVDKSCKQFTVNLSHPGNLPKNVMGHNWVLSTAADMQGVVTD
GMA**C**GLDKDYLKPDDSRVIAHTKLIGSGEKDSVTFDVSKLKEGEQYMFFCTFPGHSALMKGTL
TLK*

S78C Az DNA sequence:

GCT GAA TGC TCC GTT GAT ATC CAG GGT AAT GAT CAG
ATG CAG TTC AAC ACC AAC GCC ATC ACC GTC GAC AAG
AGC TGC AAG CAG TTC ACT GTT AAC CTG TCT CAC CCA
GGT AAC CTG CCG AAG AAC GTT ATG GGT CAC AAC TGG
GTT CTG TCC ACC GCG GCT GAC ATG CAA GGC GTT GTC
ACT GAC GGT ATG GCT AGC GGT CTG GAT AAA GAC TAC
CTG AAG CCG GAT GAC **TGC** CGA GTT ATC GCC CAC ACC
AAG CTG ATC GGA TCC GGT GAA AAA GAC TCC GTT ACT
TTC GAC GTT TCC AAG CTT AAA GAA GGT GAA CAG TAC
ATG TTC TTC TGC ACT TTC CCG GGT CAC TCC GCA CTG
ATG AAA GGT ACC CTG ACT CTG AAA TAG

S78C Az amino acid sequence:
AECSVDIQGNDQMQFNTNAITVDKSCKQFTVNLSHPGNLPKNVMGHNWVLSTAADMQGVVTD
GMASGLDKDYLKPDD**C**RVIAHTKLIGSGEKDSVTFDVSKLKEGEQYMFFCTFPGHSALMKGTL
TLK*

S100C Az DNA sequence:

GCT	GAA	TGC	TCC	GTT	GAT	ATC	CAG	GGT	AAT	GAT	CAG
ATG	CAG	TTC	AAC	ACC	AAC	GCC	ATC	ACC	GTC	GAC	AAG
AGC	TGC	AAG	CAG	TTC	ACT	GTT	AAC	CTG	TCT	CAC	CCA
GGT	AAC	CTG	CCG	AAG	AAC	GTT	ATG	GGT	CAC	AAC	TGG
GTT	CTG	TCC	ACC	GCG	GCT	GAC	ATG	CAA	GGC	GTT	GTC
ACT	GAC	GGT	ATG	GCT	AGC	GGT	CTG	GAT	AAA	GAC	TAC
CTG	AAG	CCG	GAT	GAC	TCT	CGA	GTT	ATC	GCC	CAC	ACC
AAG	CTG	ATC	GGA	TCC	GGT	GAA	AAA	GAC	TCC	GTT	ACT
TTC	GAC	GTT	**TGC**	AAG	CTT	AAA	GAA	GGT	GAA	CAG	TAC
ATG	TTC	TTC	TGC	ACT	TTC	CCG	GGT	CAC	TCC	GCA	CTG
ATG	AAA	GGT	ACC	CTG	ACT	CTG	AAA	TAG			

S100C Az amino acid sequence:
AECSVDIQGNDQMQFNTNAITVDKSCKQFTVNLSHPGNLPKNVMGHNWVLSTAADMQGVVTD
GMASGLDKDYLKPDDSRVIAHTKLIGSGEKDSVTFDV**C**KLKEGEQYMFFCTFPGHSALMKGTL
TLK*

Azurin expression and purification

Sequence-confirmed plasmids were transformed into *E. coli* BL21-DE3* competent expression cells (New England Biolabs, Ipswitch, MA). Each Az mutant was expressed and purified using slightly modified protocols from prior reports.[1,2] All growths were performed in premixed Terrific Broth (TB) media (Formedium) containing 70 mg/L carbenicillin (GoldBio Technologies). Briefly, a starter growth was shaken (200 rpm) at 37°C for 14 hours, then divided into 1 L flasks of TB with 70 mg/L carbenicillin and grown at 25°C to an OD_{600} between 1-1.3. Cells were then induced with 1 mM IPTG (GoldBio Technologies) and shaken at 25°C for 14 hours (200 rpm).

Following induction, multiple rounds of centrifugation (6200 x *g*) were used to harvest cells (Avanti J-E centrifuge, JLA-10.500 rotor). The resultant cell pellets were washed with 20 mM Tris buffer, pH 7.8, and stored at -80°C until needed. Pellets were lysed while gently shaking at room temperature for 90 minutes using 1 mg/g lysate of egg white lysozyme (GoldBio Technologies) and 0.1 mg/g lysate DNase (GoldBio Technologies) in 20 mM phosphate, pH 7.6 buffer. The lysate was centrifuged at 39,000 x *g* to remove cellular debris. The resultant supernatant was treated with 1 M sodium acetate, pH 4.5, to bring the lysate solution to ~ pH 5.0, and then excess $Cu^{II}SO_4$ was added. After a final centrifugation, the lysate was dialyzed overnight against 1 mM sodium acetate (pH 4.5). All centrifugation steps were carried out at 4°C.

CuAz variants were purified on a 5-mL, self-packed Source 15S cation exchange column (GE Amersham). CuAz was eluted around 50% eluent using a 1 - 300 mM salt gradient with sodium acetate, pH 4.5. SDS gel electrophoresis was used to assess Az purity for all mutants. Under these denaturing conditions, all Az mutants tested run as a monomer of ~14 kDa (Figure S23).

Az metal extraction and reconstitution

All Az variants were subjected to metal extraction and reconstitution with either zinc (Zn) or copper (Cu) following published protocols.[1,3,4] CuAz was first reduced with an excess of sodium

dithionite (Acros Organics) and dialyzed for three, four-hour rounds against a solution of 400 mM potassium cyanide (Alfa Aesar), buffered in 100 mM potassium phosphate at pH 8.0, resulting in the formation of apo-Az. Three, four-hour rounds of dialysis against 100 mM potassium phosphate, pH 8.0 were then performed to remove excess cyanide from apo-Az. Excess phosphate was removed via dialysis against 10 mM Tris, pH 8.0 for 4 hours. Metal reconstitution was achieved by dialysis against 7.5 mM $Cu^{II}SO_4$ or $Zn^{II}SO_4$ in 50 mM Tris, pH 7.4, for 48 hours. Excess metal was removed by buffer exchanging into 50 mM Tris, pH 8.0, using an Amicon stirred-cell concentrator (Millipore Sigma). Metal incorporation was verified using absorption spectroscopy.

RuAz generation

The bis(2,2′-bipyridine)(5,6-epoxy-5,6-dihydro-[1,10] phenanthroline) ruthenium(II) ($[Ru(bpy)_2(epoxy\text{-}phen)]^{2+}$) compound was synthesized using a procedure modified from a published protocol.[5,6] The 5,6-epoxy-5,6- dihydro-[1,10]phenanthroline ligand (14.0 mg, Santa Cruz Biotechnology) was combined with *cis*-$Ru(bpy)_2Cl_2$ (31.0 mg, Sigma-Aldrich) in a 75/25 %v/v mixture of $EtOH/H_2O$. The reaction was heated to reflux for 3 hours in the dark. The solvent was removed, and a cold, saturated solution of KPF_6 was added to crash out the desired compound ($[Ru(bpy)_2(epoxy\text{-}phen)]^{2+}$). $[Ru(bpy)_2(epoxy\text{-}phen)]^{2+}$ was collected using vacuum filtration and washed with cold deionized water. The compound purity and identity were verified using MALDI-TOF mass spectrometry.

S-to-C Az mutants were reduced with a 2.5-fold excess of dithiothreitol (DTT, Acros Organics) in 50 mM Tris buffer, pH 8.0, and allowed to incubate for 10 minutes at room temperature. Excess DTT was removed via a PD10 desalting column (Bio-Rad). $[Ru(bpy)_2(epoxy\text{-}phen)]^{2+}$ was dissolved in DMF and added to a final concentration of 100 µM to a solution of 25 µM Az in a buffer mixture of 25 mM Tris + 25 mM CHES (VWR Scientific), pH 8.5. Reactions were incubated in the dark at 37°C for 48 hours. Following incubation, the reactions were concentrated using centrifugal filter devices (Millipore Centricons, MWCO 3.5 kDa). Excess $[Ru(bpy)_2(epoxy\text{-}phen)]^{2+}$ was removed using a PD10 desalting column, and the solution was exchanged into 1 mM sodium acetate, pH 4.5, via centrifugal filtration. Ruthenium-labelled Az (RuAz) was separated from unlabelled Az via cation exchange chromatography using a 1-300 mM salt gradient with sodium acetate, pH 4.5. Fractions were collected and assessed for purity using MALDI-TOF mass spectrometry. Pure RuAz fractions were combined and exchanged into 50 mM CHES, pH 9.0. All samples were stored in the dark at 4°C until needed.

*Az-[**1**] and RuAz-[**1**] generation*

$[Ni(cyclam)]^{2+}$, ([**1**], cyclam = 1,4,8,11-tetraazacyclotetradecane) was synthesized following a published protocol.[7] Cyclam (Acros Organics) was dissolved in ethanol and combined in a 1:1 molar ratio with $Ni^{II}Cl_2*6H_2O$ (Alfa Aesar). The resulting mauve solution was heated slightly to 37 ˚C and stirred for 15 minutes. [**1**]Cl_2 was precipitated upon the addition of diethyl ether and collected by vacuum filtration. To generate RuAz-[**1**], RuAz was incubated while shaking in the dark at 37°C (48 hours, 70 rpm) with a ten-fold molar excess of [**1**] in 50 mM CHES, pH 9.0. Excess [**1**] was removed via a PD10 desalting column (Bio-Rad) immediately prior to use. If necessary, samples were concentrated using centrifugal filter devices.

UV-Vis spectroscopy

All UV-visible absorption spectra were collected on a Shimadzu UV-2600 spectrophotometer.

Electrochemistry experiments

All cyclic voltammetry (CV) electrochemistry experiments were conducted using a CHI 760E potentiostat (CH Instruments). A typical three-electrode set up was employed for solution-phase electrochemistry, with a 3 mm glassy carbon working electrode (CH Instruments), a platinum wire counter electrode, and a mini Ag/AgCl (sat. KCl) reference electrode (Pine Instruments). Prior to

each experiment, the glassy carbon working electrode was polished for 60 seconds with 1.0 micron alumina powder, extensively rinsed with deionized water, then polished for 60 seconds with 0.05 micron alumina powder (CH Instruments). The electrode was rinsed again and sonicated for three minutes. Potentials were reported against NHE by the addition of +198 mV to the experimentally measured potentials.

Light-driven catalytic assays

The experimental conditions for the $[Ru^{II}(bpy)_3]^{2+}$ assay were adapted from previously published protocols.[8] All assays were performed in a home-made cell with circulating, chilled water at 4°C. The average pathlength for photoexcitation within this cell is 1.8 cm. Assays were carried out under a CO_2 atmosphere in a mixed buffer system of 12.5 mM CHES, pH 9.0 + 750 mM phosphate, pH 8.0, giving a final pH of 7.25 because of the dissolved CO_2. A strong dependence of activity on the RuAz-[**1**] stock concentration was observed; as such, RuAz-[**1**] stocks of 50 μM concentration were diluted for assays. Each assay contained 5 μM RuMAz-[**1**] (based on Ru) and 100 mM ascorbate (Sigma-Aldrich), unless otherwise noted. For experiments requiring CO_2, buffers were extensively sparged before use with a high-purity carbon dioxide gas cylinder (Praxair) and were left under a saturated CO_2 atmosphere. For photoexcitation, four LUXEON Rebel ES LEDs (447.5 nm) were spaced under the chiller set up, directly below the septum-capped GC vials. To quantify product formation, headspace samples were removed using a Hamilton gas-tight syringe and injected into the gas chromatograph for analysis. Assays were performed in triplicate and results are reported as the average with standard deviations.

Gas chromatography analysis

Gas chromatography analysis was performed using a Shimadzu GC-2014 fuel cell analyzer system equipped with a thermal conductivity detector and a flame ionization detector coupled to a methanizer. Argon was used as the carrier gas for all experiments. Separation was achieved using a temperature gradient with the use of the following columns: HayeSep-N (3 m, 80/100 mesh), HayeSep-T (2 m, 80/100 mesh), Shimalite Q (0.2 m, 100/180), Shimalite Q (0.25 m, 100/180), Shimalite Q (0.15 m, 100/180), and a 5-Ångstrom molecular sieve (2.5 m, 60/80). Standard curves were generated using injections of Scotty standard gas calibration mixture (Figure S24, Product #A0908910)

MALDI-TOF mass spectrometry analysis

All protein samples were desalted using Micro-C_{18} Millipore Ziptips (Sigma-Aldrich) prior to analysis and prepared on a ground steel plate (Bruker MSP 96 microScout Target). A final concentration of approximately 25 μM protein was used for analysis. The matrix was composed of 200 mM sinapic acid (Sigma-Aldrich) in 30 mM ammonium citrate and 30% acetonitrile. Following a 1:1 dilution with matrix, the sample/matrix mixture was allowed to dry on the plate overnight before analysis. Samples were analyzed on a Bruker microFlex MALDI-TOF instrument.

Luminescence and TCSPC studies

All samples were prepared in an anaerobic glovebox (Vigor Technologies) into septum-capped 1 x 0.2 cm cuvettes (FireflySci). Samples were prepared to a final concentration of 5 μM ruthenium. Experiments were carried out under a saturated CO_2 atmosphere in a mixed buffer system of 750 mM PO_4/12.5 mM CHES, pH 7.25. Following sample preparation, each sample was analyzed using UV-Vis spectroscopy to obtain an accurate concentration measurement. Emission spectral intensities were corrected for small variations in concentration. Emission spectra were collected on an Horiba Scientific Fluoro-Max-4 spectrofluorometer using a sample excitation wavelength of 450 nm, monitoring emission from 475-850 nm. TCSPC analysis was performed on each sample using an Edinburgh Instruments EPL-445 instrument equipped with a 444.4 nm laser giving 84.4 ps pulses for excitation. This system was coupled to an Edinburgh

Instruments mini-τ TCSPC detector to monitor photons emitted. The luminescence was monitored in the range of 577.5-622.5 nm using a band-pass filter.

For Stern-Volmer quenching analysis, similar sample preparation protocols were used; however, varying amounts of sodium ascorbate (Asc, Sigma-Aldrich), sodium dithionite (DT, Acros Organics), sodium diethyldithiocarbamate (DTC, Sigma-Aldrich), or 4-methoxy-N,N-dimethylaniline (*p*-MeODMA, OxChem) were added as indicated. Each quencher was prepared fresh, immediately prior to experimentation. To prepare a 25 mM aqueous stock solution of *p*-MeODMA, *p*-MeODMA was dissolved in EtOH and diluted to the desired concentrations using phosphate buffer. NOTE: Aqueous stocks of *p*-MeODMA at concentrations greater than approximately 25 mM were insoluble.

Quantum yield analysis

To determine quantum yields of all samples, a potassium ferrioxalate actinometer assay was used. The experiment was adapted from previous reports.[9–11] Briefly, a 0.150 M potassium ferrioxalate trihydrate (Strem Chemicals, Inc.) solution was prepared in 0.05 M H_2SO_4. A 0.2 % 1,10-phenanthroline (Sigma-Aldrich) solution was prepared in 1.64 M sodium acetate and 0.5 M H_2SO_4 and was then diluted 10 fold. The ferrioxalate solution was diluted 10 fold and samples were irradiated for periods of 2.5, 5, or 7.5 seconds. Following irradiation, the samples were diluted two-fold with the diluted phenanthroline solution and incubated for 10 minutes. Sample absorbance was monitored at 510 nm using UV-vis spectroscopy (ε_{510} = 1.1 x 10^4 M^{-1} cm^{-1}) to determine the concentration of the $[Fe(phen)_3]^{2+}$ formed. Sample absorbance was corrected by subtracting the corresponding dark control. Given the reported quantum yield for photoactivity of 0.93 at 447 nm, a photon flux of 1.12 x 10^{17} photons/s was calculated. These measurements were repeated in triplicate.

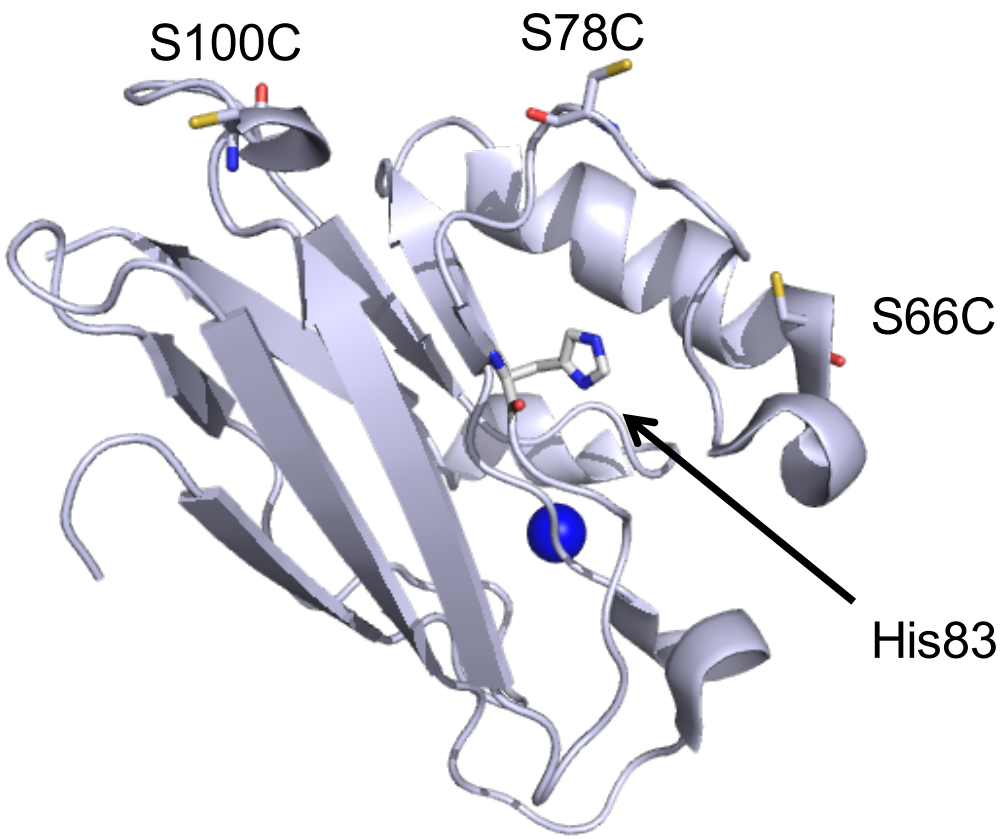

S66C-Metal	S78C-Metal	S100C-Metal
16.1 Å	23.4 Å	29.1 Å
S66C-His83	**S78C-His83**	**S100C-His83**
11.2 Å	11.8 Å	19.3 Å

Figure S1. Structure of Az (PDB: 4AZU) with cysteine labeling sites and histidine-83 indicated. All cysteine residues were modeled with the Pymol mutagenesis wizard using the same conformation as the native serine residue. Indicated distances reflect the estimated separation between the Cys sulfur atom to either the Cu metal center (S->C – Metal) or His-Nε atom (S->C – His83).

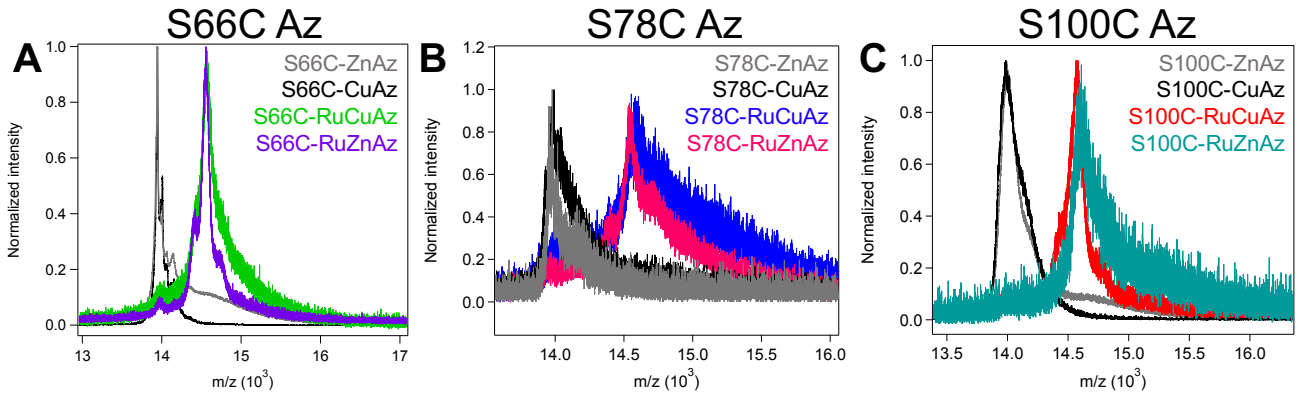

Figure S2. MALDI-TOF analysis of RuMAz vs. MAz for the indicated samples. Sample intensities were normalized to facilitate direct comparison.

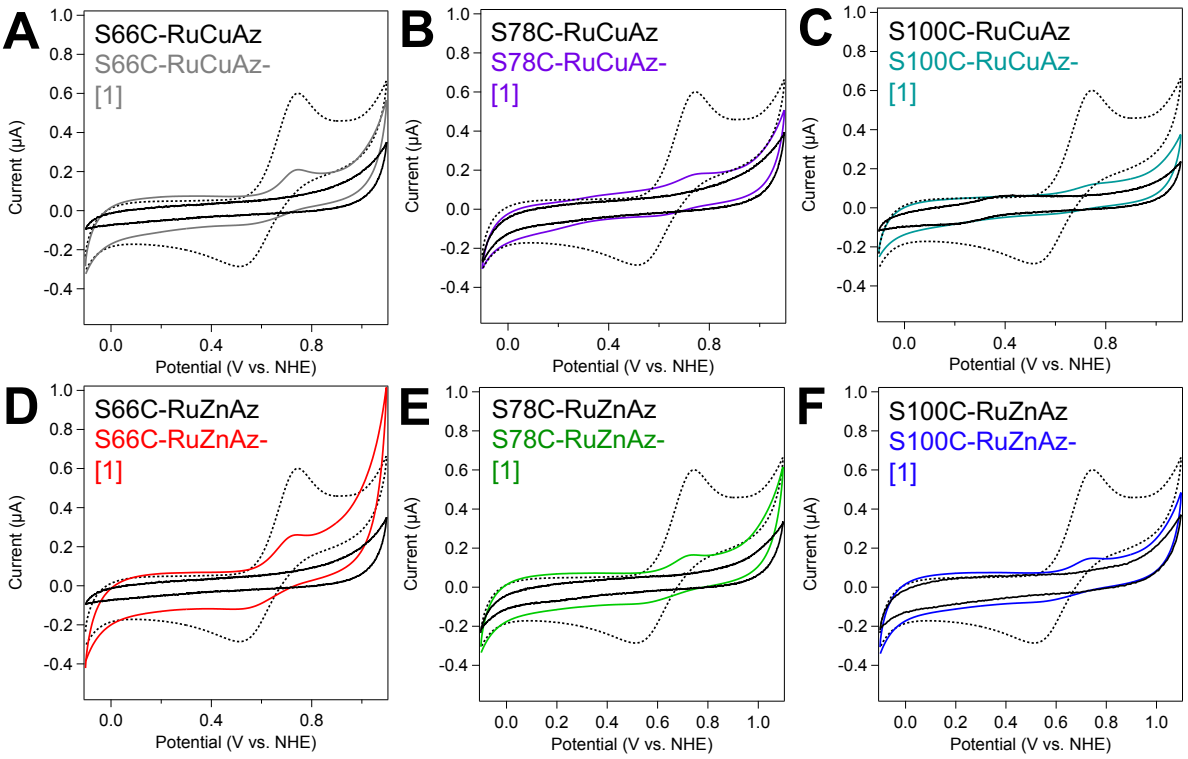

Figure S3. Cyclic voltammograms of RuMAz vs. RuMAz-[**1**]. All samples contained 150 μM RuMAz in 37.5 mM phosphate/12.5 mM CHES buffer, pH 7.25, with 100 mM KCl. Pure RuMAz controls displayed in black; the cyclic voltammogram of free [**1**] in solution is overlaid on all voltammograms as a dotted black line.

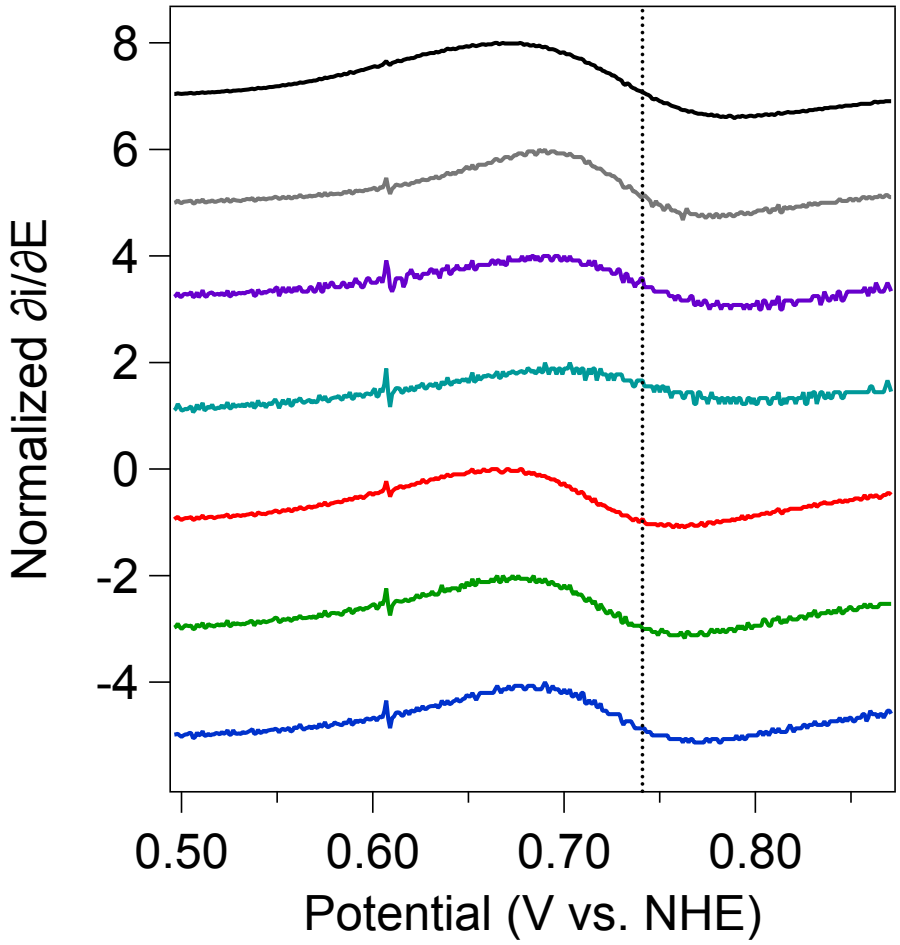

Figure S4. Normalized first-derivative traces of cyclic voltammograms of [**1**] in solution (black), S66C-RuCuAz-[**1**] (gray), S78C-RuCuAz-[**1**] (purple), S100C-RuCuAz-[**1**] (teal), S66C-RuZnAz-[**1**] (red), S78C-RuZnAz-[**1**] (green), and S100C-RuZnAz-[**1**] (blue). All samples contained 150 μM catalyst in 37.5 mM phosphate/12.5 mM CHES buffer, pH 7.25, with 100 mM KCl.

Table S1. $Ni^{III/II}$ reduction potentials and peak separation.

Sample	$Ni^{III/II}$ Reduction Potential (mV vs. NHE)	$Ni^{III/II}$ Peak Separation (mV)
S66C-RuZnAz-[**1**]	640	170
S78C-RuZnAz-[**1**]	645	155
S100C-RuZnAz-[**1**]	655	170
S66C-RuCuAz-[**1**]	670	140
S78C-RuCuAz-[**1**]	700	100
S100C-RuCuAz-[**1**]	690	135
[**1**]	636	215

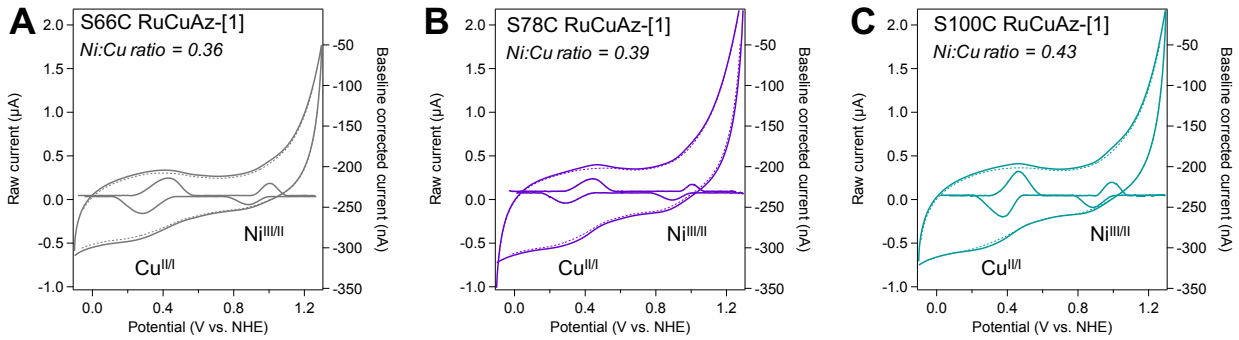

Figure S5. Cyclic voltammograms of RuCuAz-[**1**]. All samples contained 150 μM RuCuAz-[**1**] in 35 mM sodium acetate/15 mM CHES buffer, pH 4.5, with 100 mM KCl. Samples were diluted into acetate buffer immediately prior to electrochemical analysis to retain the Az-[**1**] bond throughout the experiment. A capacitative current baseline (dashed line) was subtracted from the cyclic voltammograms in QSOAS to isolate the Faradaic contribution and quantify relative incorporation of [**1**] into the protein.

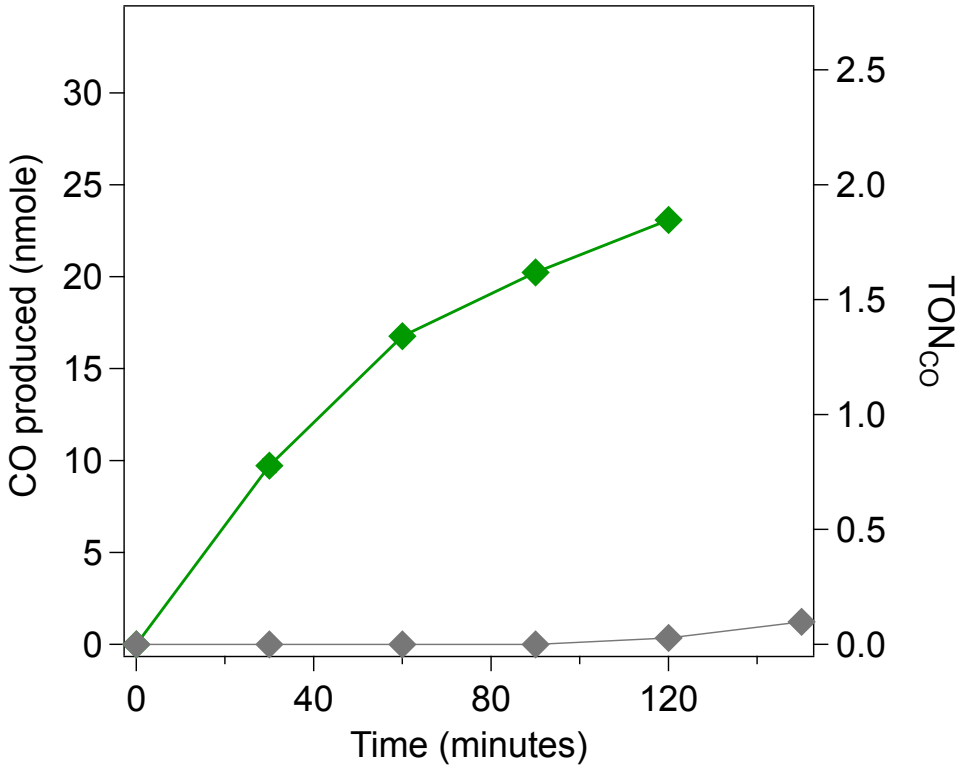

Figure S6. Control GC photoassay of S78C-RuCuAz-[**1**] (green) and S78C-RuCuAz (gray) showing CO produced following irradiation (λ_{ex} = 447.5 nm). Samples contained 5 μM RuCuAz in 750 mM phosphate/12.5 mM CHES buffer with 100 mM ascorbate, pH 7.25, under a CO_2 atmosphere.

Table S2. Measured GC peak areas for CO detection following 2 hours (or 2.5 hours for S78C-RuCuAz control) of irradiation and corresponding total nmoles produced when scaled for injection volume relative to headspace volume. Samples contained 5 μM protein in 750 mM phosphate/12.5 mM CHES buffer, pH 7.25, with 100 mM ascorbate under a CO_2 atmosphere unless otherwise specified.

Sample	Measured CO area	CO (total nmoles)
S78C-RuCuAz-[**1**]	36350	23.1
S78C-RuCuAz	480	0.3
S78C-RuCuAz-[**1**] - Asc	100	0.05
S78C-RuCuAz-[**1**] - light	205	0.1
S78C-RuCuAz-[**1**] - CO_2	750	0.5

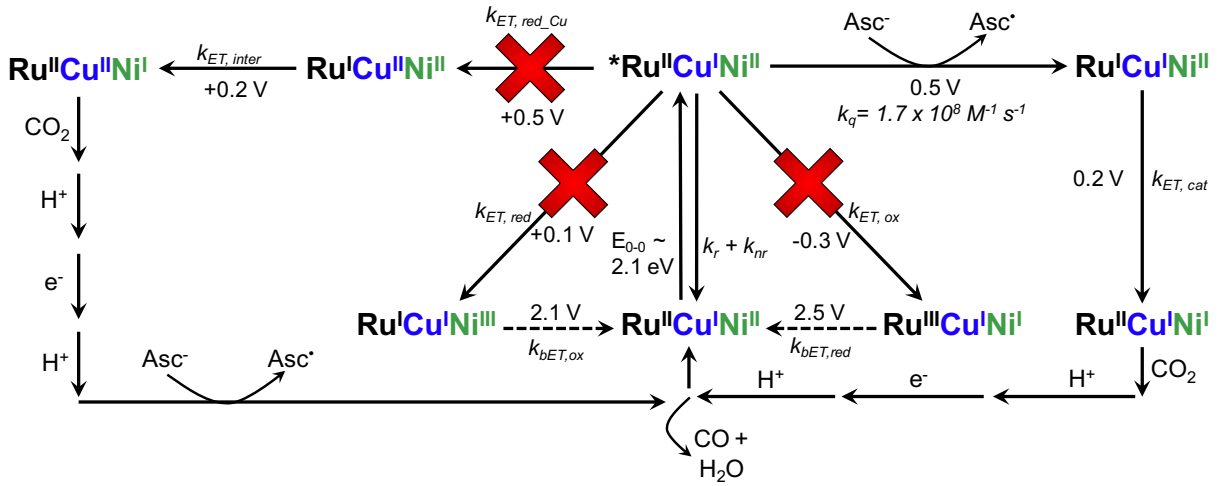

Figure S7. Modified Latimer diagram for ET processes in RuCuAz-[**1**]. The ascorbate present in solution reduces the Cu^{II}Az center to Cu^{I}Az prior to initiation of the assay. Reduction potentials for Ru,[12] CuAz,[1] and [**1**][2] taken from literature. Possible routes for excited-state quenching that are not observed in this work indicated on diagram.

Table S3. Quantum yields for CO produced by RuMAz-[**1**] and $[Ru(bpy)_3]^{2+}$ + [**1**] following 2 hours of irradiation at 447.5 nm.

Sample	Quantum yield
S66C-RuZnAz-[**1**]	9.3×10^{-5}
S78C-RuZnAz-[**1**]	1.1×10^{-4}
S100C-RuZnAz-[**1**]	6.9×10^{-5}
S66C-RuCuAz-[**1**]	9.9×10^{-5}
S78C-RuCuAz-[**1**]	1.4×10^{-4}
S100C-RuCuAz-[**1**]	8.3×10^{-5}
$[Ru(bpy)_3]^{2+}$ + [**1**]	1.8×10^{-4}

A

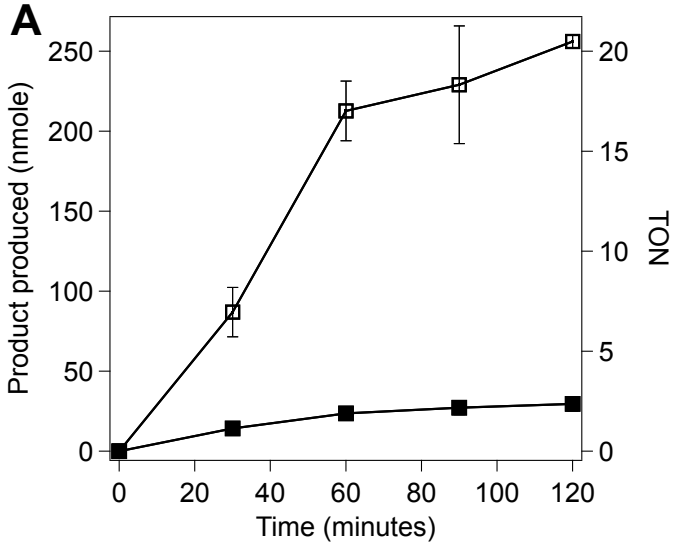

B

Time (minutes)	SR (CO/H_2)
0	0
30	0.16
60	0.1
90	0.12
120	0.12

Figure S8. GC photoassay of 5 μM $[Ru(bpy)_3]^{2+}$ + 5 μM [**1**] in 750 mM phosphate/12.5 mM CHES, pH 7.25, with 100 mM ascorbate under a CO_2 atmosphere. (**A**) GC quantitation of product produced following irradiation with 447.5 nm light. Error bars represent standard deviations from measurements performed in triplicate. Closed squares represent CO produced while open squares represent hydrogen production. (**B**) Table of selectivity ratios (SR) vs. time.

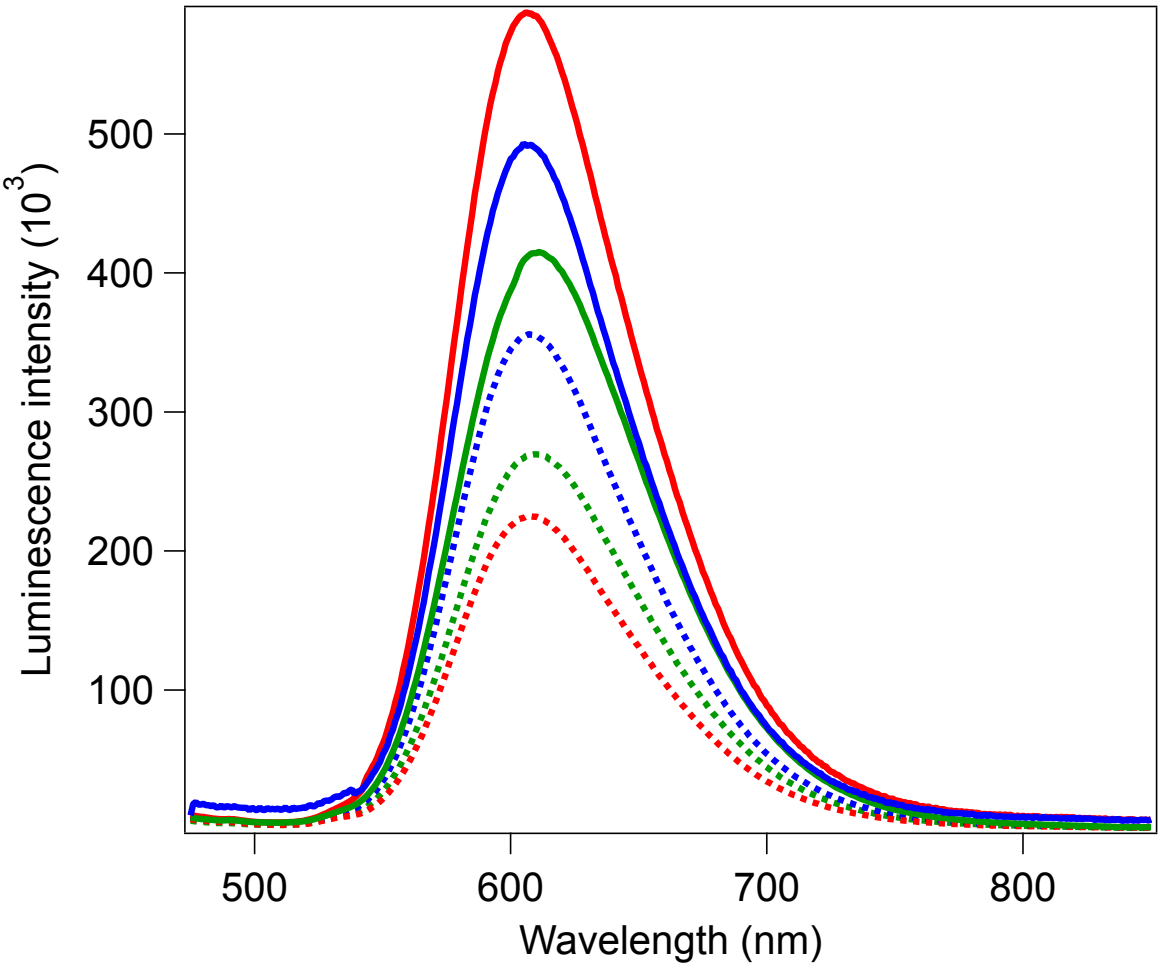

Figure S9. Emission spectra of S100C-RuMAz (blue), S78C-RuMAz (green), and S66C-RuMAz (red) for M = Zn (solid lines) and Cu (dashed lines). Samples contained 5 μM RuMAz in 750 mM phosphate/12.5 mM CHES, pH 7.25 under a CO_2 atmosphere. Intensities were normalized for Ru concentration.

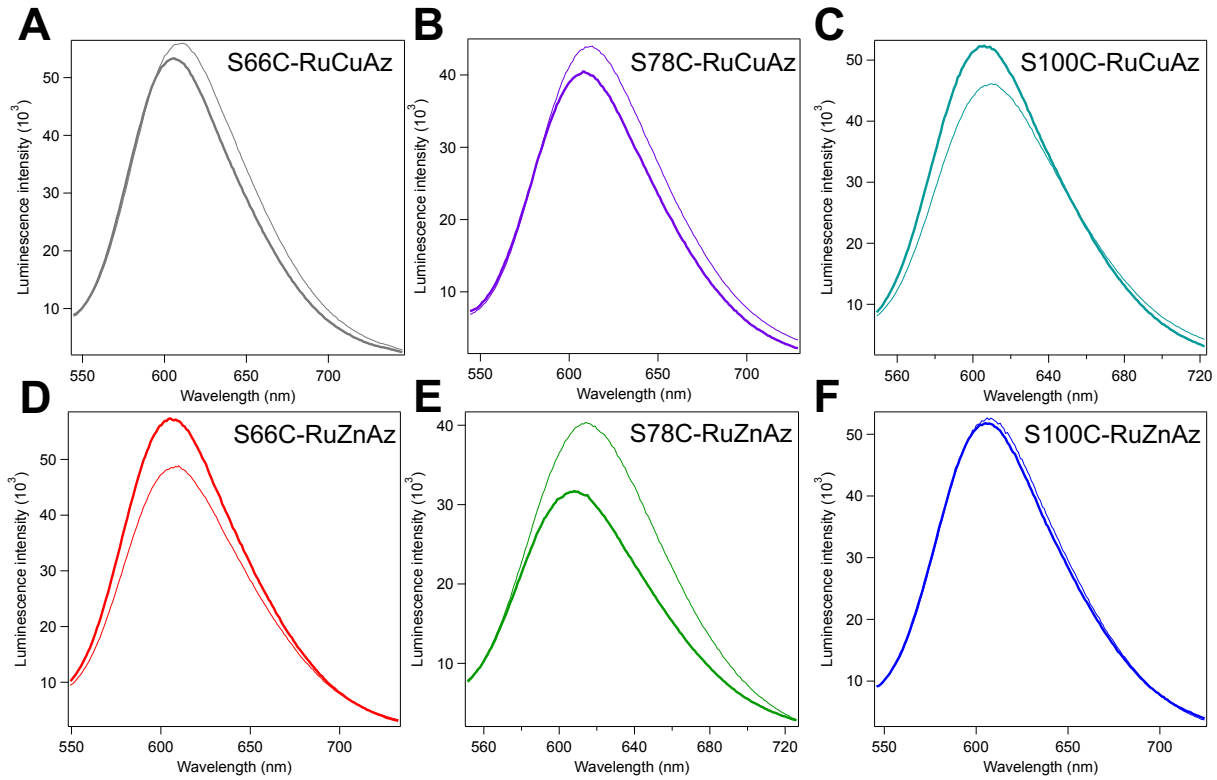

Figure S10. Luminescence spectra of RuMAz (thin lines) vs. RuMAz-[**1**] (thick lines) under catalytic conditions. All samples contained 5 μM RuMAz in 750 mM phosphate/12.5 mM CHES, pH 7.25, in the presence of 100 mM ascorbate under an atmosphere of CO_2. Specific variants indicated on figure panels. Intensities were normalized for Ru concentration.

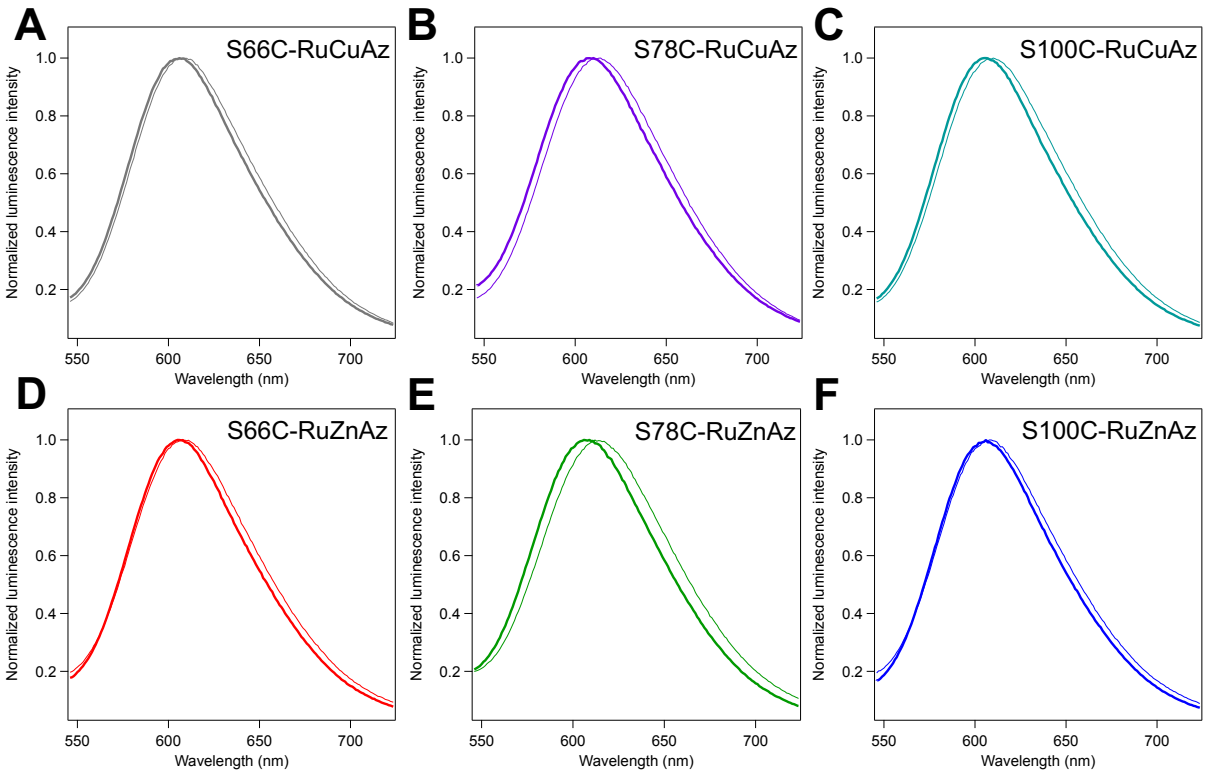

Figure S11. Normalized luminescence spectra of RuMAz (thin lines) vs. RuMAz-[**1**] (thick lines) under catalytic conditions. All samples contained 5 μM RuMAz in 750 mM phosphate/12.5 mM CHES, pH 7.25, in the presence of 100 mM ascorbate under an atmosphere of CO_2. Specific variants indicated on figure panels. Intensities were normalized for direct comparison of emission wavelengths.

Table S4. Peak emission wavelengths for each sample.

Sample	Peak emission wavelength (nm)
S66C-RuZnAz	608
S66C-RuZnAz-[**1**]	606
S78C-RuZnAz	614
S78C-RuZnAz-[**1**]	608
S100C-RuZnAz	608
S100C-RuZnAz-[**1**]	606
S66C-RuCuAz	608
S66C-RuCuAz-[**1**]	606
S78C-RuCuAz	614
S78C-RuCuAz-[**1**]	608
S100C-RuCuAz	610
S100C-RuCuAz-[**1**]	606
$[Ru(bpy)_3]^{2+}$	606
$[Ru(bpy)_3]^{2+}$ + [**1**]	606

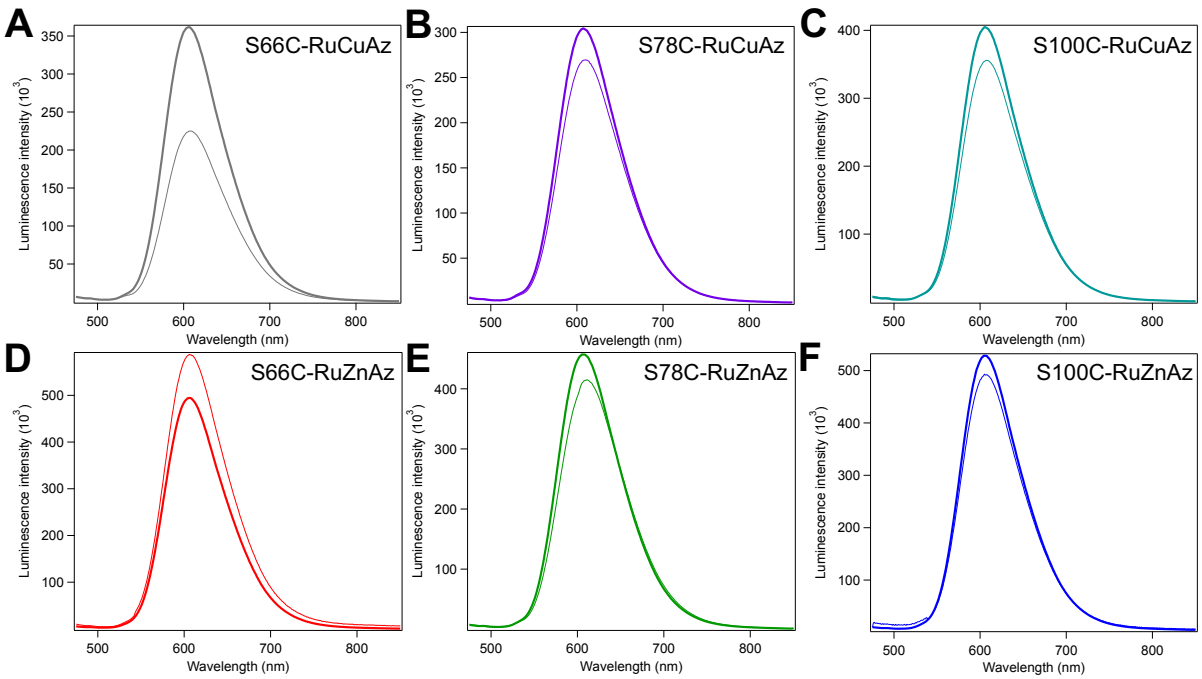

Figure S12. Luminescence spectra of RuMAz (thin lines) vs. RuMAz-[**1**] (thick lines) under non-catalytic conditions. All samples contained 5 μM RuMAz in 750 mM phosphate/12.5 mM CHES, pH 7.25, under an atmosphere of CO_2. Specific variants indicated on figure panels. Intensities were normalized for Ru concentration.

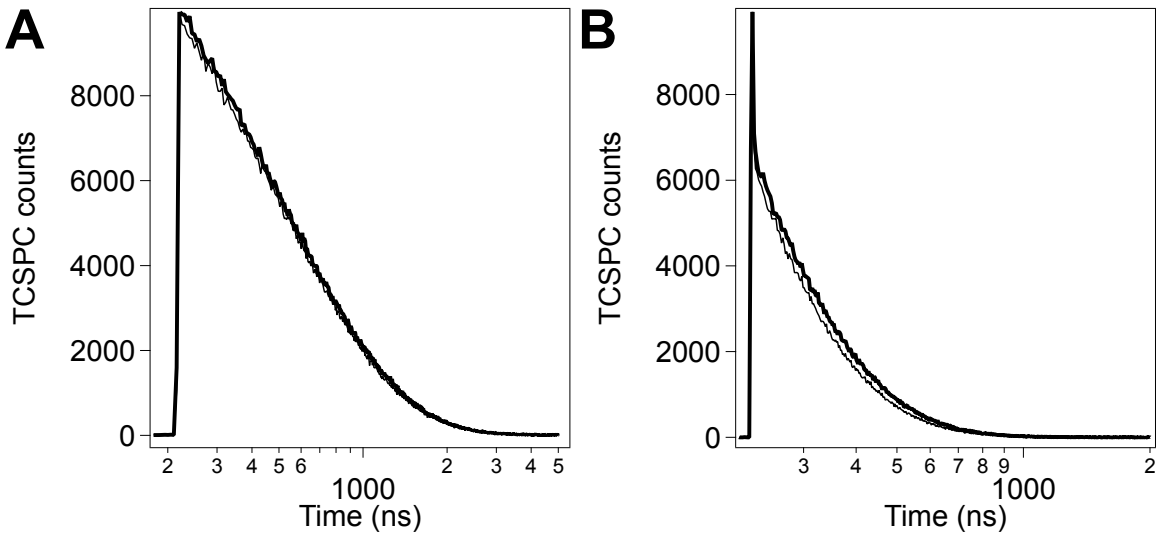

Figure S13. TCSPC decay traces of $[Ru(bpy)_3]^{2+}$ (thin lines) vs $[Ru(bpy)_3]^{2+}$ + 1 eq. [**1**] (thick lines) for (**A**) 5 μM $[Ru(bpy)_3]^{2+}$ in 750 mM phosphate/12.5 mM CHES, pH 7.25 and (**B**) 5 μM $[Ru(bpy)_3]^{2+}$ in 750 mM phosphate/12.5 mM CHES, pH 7.25, in the presence of 100 mM ascorbate as a reductive quencher. All experiments performed under a CO_2 atmosphere.

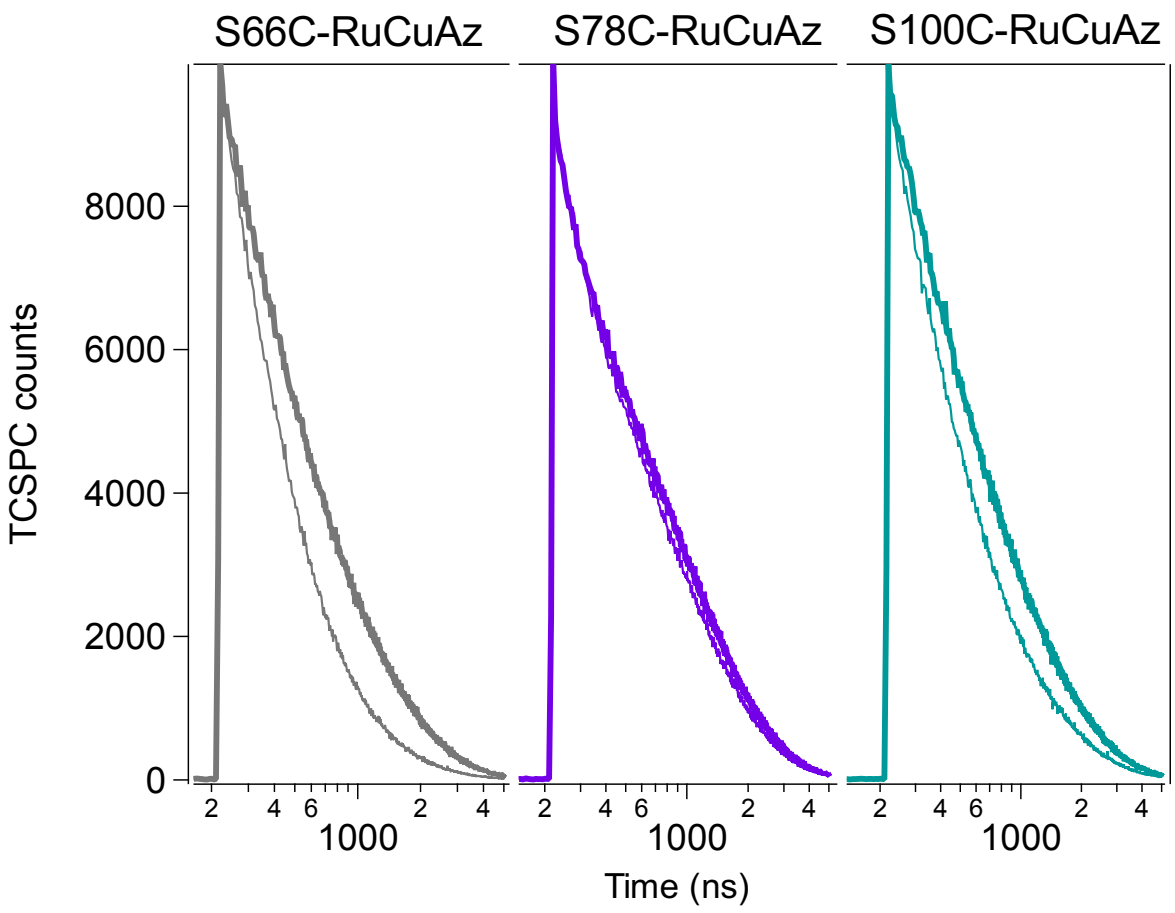

Figure S14. TCSPC decay traces of RuCuAz (thin lines) vs. RuCuAz-[**1**] (thick lines) under non-catalytic conditions. Samples contained 5 μM RuCuAz in 750 mM phosphate/12.5 mM CHES, pH 7.25, with the specific variants indicated on figure labels. All experiments performed under a CO_2 atmosphere.

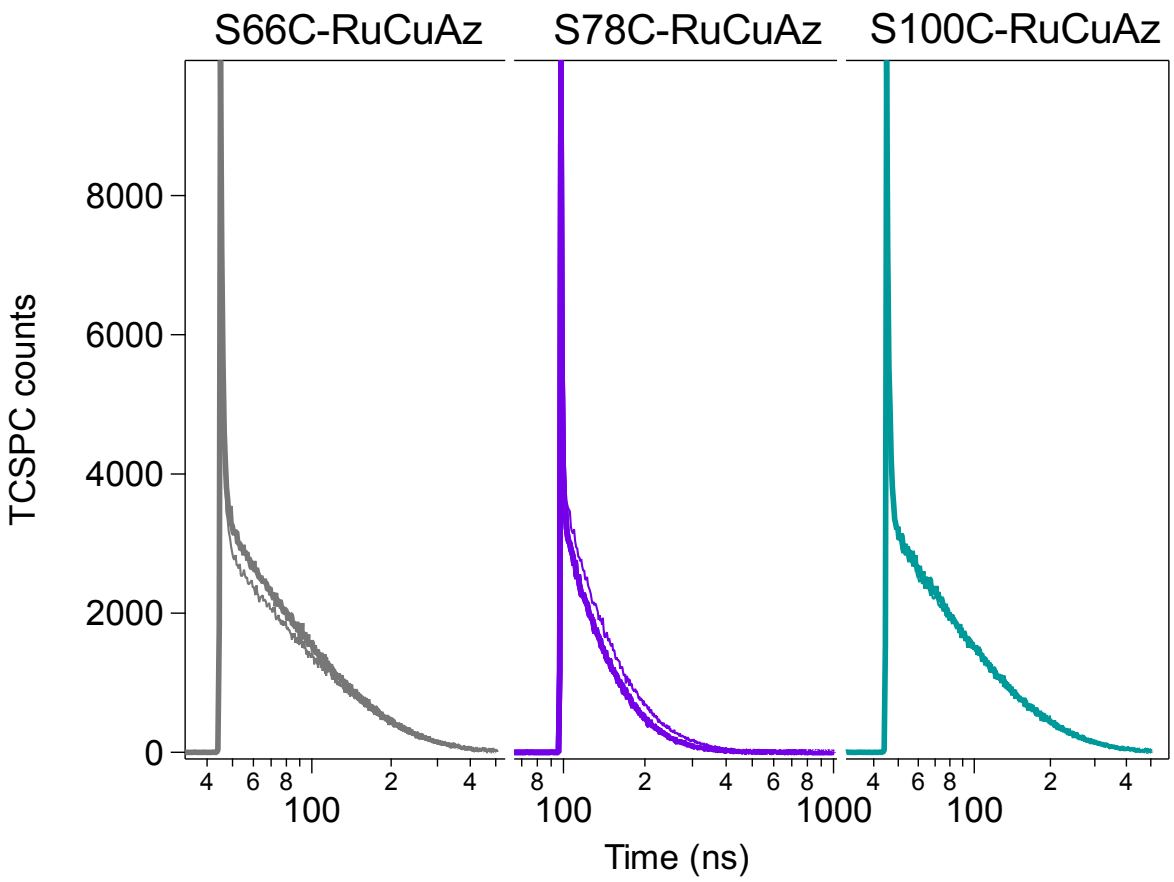

Figure S15. TCSPC decay traces of RuCuAz (thin lines) vs. RuCuAz-[**1**] (thick lines) under catalytic conditions. Samples contained 5 μM RuCuAz in 750 mM phosphate/12.5 mM CHES, pH 7.25, in the presence of 100 mM ascorbate; specific variants are indicated on figure labels. All experiments performed under a CO_2 atmosphere.

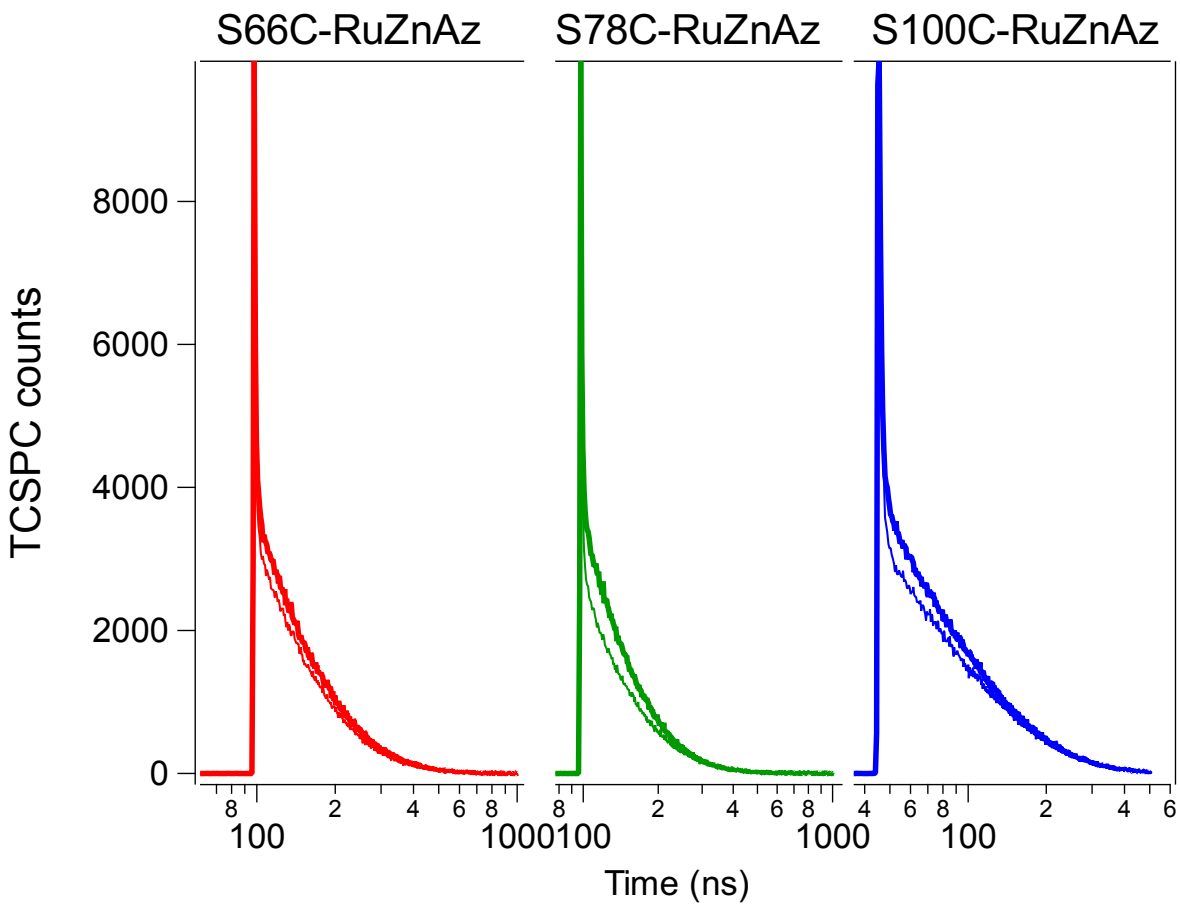

Figure S16. TCSPC decay traces of RuZnAz (thin lines) vs. RuZnAz-[**1**] (thick lines) under catalytic conditions. Samples contained 5 μM RuZnAz in 750 mM phosphate/12.5 mM CHES, pH 7.25, in the presence of 100 mM ascorbate; specific variants are indicated on figure labels. All experiments performed under a CO_2 atmosphere.

Table S5. TCSPC lifetimes from exponential fits with number of components indicated for RuMAz and RuMAz-[**1**] under non-catalytic conditions. Samples contained 5 μM RuMAz or $[Ru(bpy)_3]^{2+}$ in 750 mM phosphate/12.5 mM CHES, pH 7.25, under a CO_2 atmosphere. Reported errors are standard deviations from n=3 replicates.

Sample	τ_1 (ns)	A_1 (%)	τ_2 (ns)	A_2 (%)	τ_3 (ns)	A_3 (%)	Weighted τ (ns)
$[Ru(bpy)_3]^{2+}$	494 ± 11	100	NA	NA	NA	NA	494 ± 11
$[Ru(bpy)_3]^{2+}$ + [**1**]	492 ± 26	100	NA	NA	NA	NA	492 ± 26
S66C-RuCuAz	57 ± 25	9 ± 2	240 ± 22	61 ± 6	820 ± 50	31 ± 4	400 ± 50
S66C-RuCuAz-[**1**]	20 ± 8	17 ± 12	250 ± 7	42 ± 10	973 ± 70	42 ± 7	515 ± 80
S78C-RuCuAz	30 ± 30	10 ± 10	265 ± 2	20 ± 4	915 ± 70	70 ± 6	692 ± 11
S78C-RuCuAz-[**1**]	10 ± 5	8 ± 5	84 ± 6	54 ± 5	850 ± 50	39 ± 10	372 ± 56
S100C-RuCuAz	20 ± 20	20 ± 13	240 ± 25	47 ± 8	890 ± 90	34 ± 5	425 ± 100
S100C-RuCuAz-[**1**]	20 ± 20	6 ± 3	253 ± 29	36 ± 6	943 ± 50	58 ± 5	640 ± 58
S66C-RuZnAz	252 ± 6	14 ± 1	1035 ± 35	86 ± 1	NA	NA	927 ± 33
S66C-RuZnAz-[**1**]	167 ± 53	8 ± 1	980 ± 92	92 ± 1	NA	NA	918 ± 83
S78C-RuZnAz	253 ± 36	28 ± 5	897 ± 63	72 ± 5	NA	NA	716 ± 73
S78C-RuZnAz-[**1**]	185 ± 75	10 ± 2	955 ± 40	90 ± 2	NA	NA	886 ± 28
S100C-RuZnAz	230 ± 30	12 ± 1	990 ± 50	88 ± 1	NA	NA	900 ± 40
S100C-RuZnAz-[**1**]	200 ± 70	9 ± 1	1028 ± 30	91 ± 1	NA	NA	955 ± 35

Table S6. TCSPC lifetimes from exponential fits with number of components indicated for RuMAz and RuMAz-[**1**] under catalytic conditions. Samples contained 5 μM RuMAz or $[Ru(bpy)_3]^{2+}$ in 750 mM phosphate/12.5 mM CHES, pH 7.25, with 100 mM ascorbate under a CO_2 atmosphere.

Sample	τ_1 (ns)	A_1 (%)	τ_2 (ns)	A_2 (%)	τ_3 (ns)	A_3 (%)	Weighted τ (ns)
$[Ru(bpy)_3]^{2+}$	1 ± 1	25 ± 8	135 ± 6	75 ± 8	NA	NA	100 ± 10
$[Ru(bpy)_3]^{2+}$ + [**1**]	2 ± 1	30 ± 10	138 ± 1	71 ± 12	NA	NA	100 ± 17
S66C-RuCuAz	57 ± 24	65 ± 1	30 ± 30	13 ± 10	95 ± 20	23 ± 10	27 ± 2
S66C-RuCuAz-[**1**]	1 ± 1	64 ± 3	25 ± 7	7 ± 1	84 ± 2	29 ± 3	26 ± 1
S78C-RuCuAz	1 ± 0.2	25 ± 2	31 ± 3	20 ± 20	71 ± 1	50 ± 1	44 ± 2
S78C-RuCuAz-[**1**]	1± 0.2	31 ± 9	25 ± 25	24 ± 21	66 ± 15	45 ± 30	36 ± 1
S100C-RuCuAz	1 ± 0.1	20 ± 20	23 ± 20	17 ± 6	85 ± 4	64 ± 25	58 ± 15
S100C-RuCuAz-[**1**]	1 ± 0.1	50 ± 20	24 ± 10	10 ± 6	81 ± 4	40 ± 15	35 ± 13
S66C-RuZnAz	1 ± 0.1	71 ± 3	76 ± 4	30 ± 3	NA	NA	23 ± 3
S66C-RuZnAz-[**1**]	1 ± 0.2	70 ± 2	78 ± 3	31 ± 2	NA	NA	25 ± 2
S78C-RuZnAz	2 ± 1	63 ± 3	74 ± 1	37 ± 4	NA	NA	29 ± 3
S78C-RuZnAz-[**1**]	1 ± 0.3	66 ± 3	66 ± 3	34 ± 3	NA	NA	23 ± 1
S100C-RuZnAz	1 ± 0.2	69 ± 5	78 ± 2	31 ± 5	NA	NA	25 ± 3
S100C-RuZnAz-[**1**]	1 ± 0.2	60 ± 10	73 ± 1	91 ± 1	NA	NA	30 ± 8

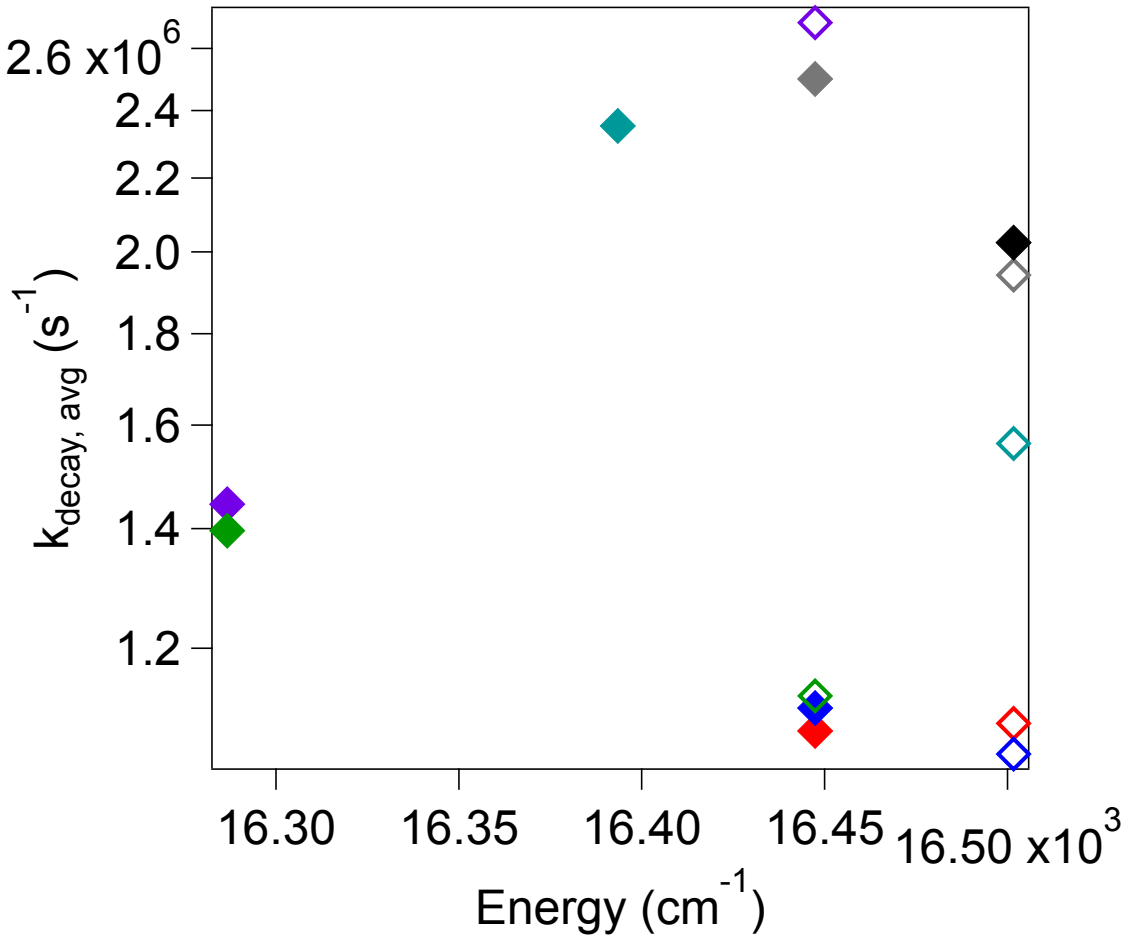

Figure S17. Energy gap law analysis showing average rates of radiative decay ($k_{decay,avg}$) vs. emission energy for RuMAz (closed diamonds) and RuMAz-[**1**] (open diamonds) for the following samples: S66C-RuCuAz (gray), S78C-RuCuAz (purple), S100C-RuCuAz (teal), S66C-RuZnAz (red), S78C-RuZnAz (green), S100C-RuZnAz (blue), and $[Ru^{II}(bpy)_3]^{2+}$ (black). The deviation from a simple linear trend suggest multiple factors may contribute to the shifts in emission wavelength and also indicate that considering average emission lifetimes may not be an accurate method to assess this correlation. Time-resolved absorption spectra and/or ultrafast techniques will be needed to separate radiative from non-radiative decay rates.

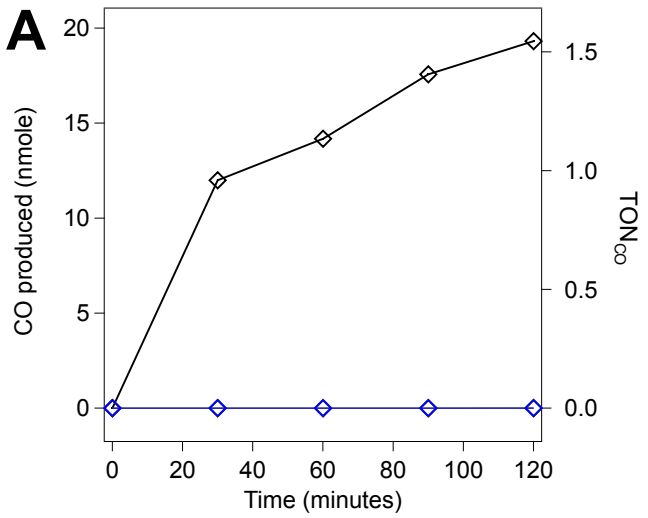

B

Quencher	CO produced (nmole)
Asc	16.3
DT	0.05
DTC	0.05
p-MeODMA	0.05

Figure S18. GC assays of S78C-RuZnAz-[**1**] using different reducing agents as sacrificial electron donors. Samples contained 5 μM S78C-RuZnAz-[**1**] in 750 mM phosphate/12.5 mM CHES buffer, pH 7.25, with 100 mM of the following quenchers: ascorbate (black), DT (blue), DTC (green), and 18.75 mM *p*-MeODMA (pink). (**A**) Graph showing CO produced under all four conditions. (**B**) Tabulated values of CO produced (total nmoles) after 2 hrs by S78C-RuZnAz-[**1**] using the indicated sacrificial electron donors.

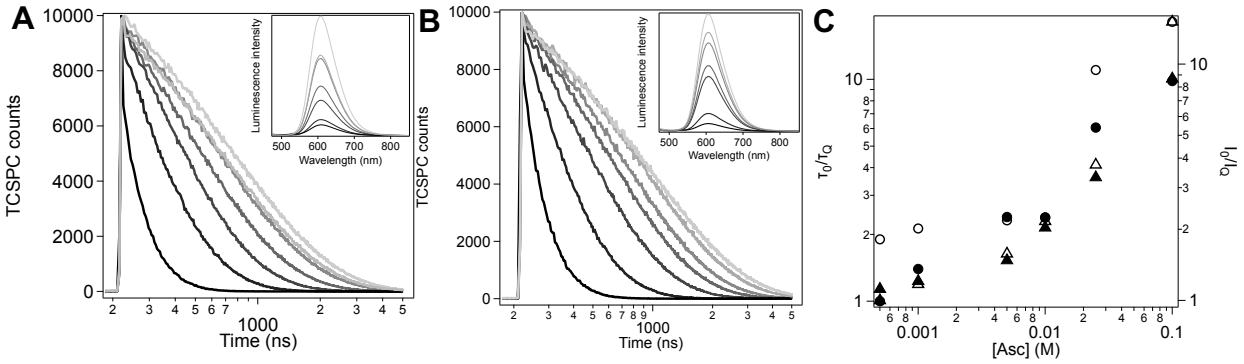

Figure S19. Stern-Volmer quenching analysis of S78C-RuZnAz vs. S78C-RuZnAz-[**1**] with ascorbate. (**A**) TCSPC decay traces of S78C-RuZnAz and (*inset*) corresponding luminescence spectra. (**B**) TCSPC traces of S78C-RuZnAz-[**1**] and (*inset*) corresponding luminescence spectra. (**C**) Stern-Volmer plot of S78C-RuZnAz (closed markers) vs. S78C-RuZnAz-[**1**] (open markers) using both I_0/I_Q (circles) and τ_0/τ_Q (triangles) ratios for analysis. Samples contained 5 μM RuZnAz in 750 mM phosphate/12.5 mM CHES buffer, pH 7.25, in the presence of 0, 0.5, 1, 5, 10, 25, and 100 mM ascorbate. All experiments performed under a CO_2 atmosphere. Luminescence spectral intensities were normalized to Ru concentration.

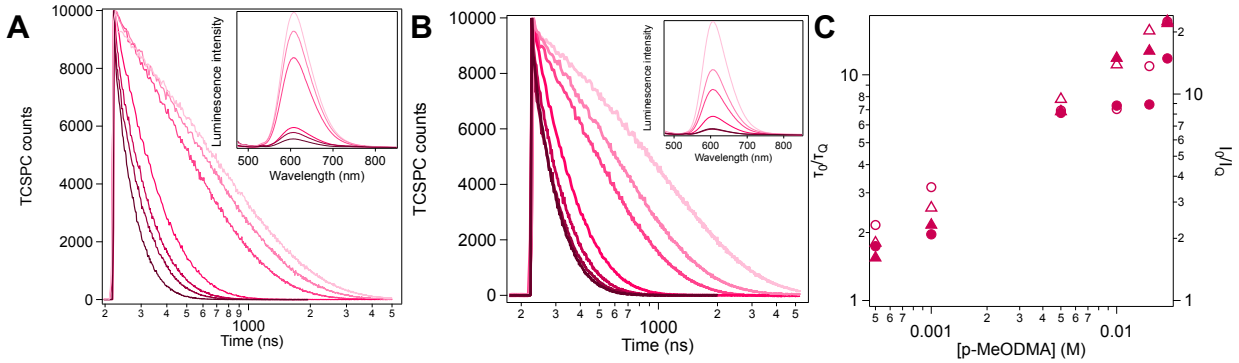

Figure S20. Stern-Volmer quenching analysis of S78C-RuZnAz vs. S78C-RuZnAz-[**1**] with *p*-MeODMA. (**A**) TCSPC decay traces of S78C-RuZnAz and (*inset*) corresponding luminescence spectra. (**B**) TCSPC traces of S78C-RuZnAz-[**1**] and (*inset*) corresponding luminescence spectra. (**C**) Stern-Volmer plot of S78C-RuZnAz (closed markers) vs. S78C-RuZnAz-[**1**] (open markers) using both I_0/I_Q (circles) and τ_0/τ_Q (triangles) ratios for analysis. Samples contained 5 μM RuZnAz in 750 mM phosphate/12.5 mM CHES buffer, pH 7.25, in the presence of 0, 0.5, 1, 5, 10, 15, and 18.75 mM *p*-MeODMA. All experiments performed under a CO_2 atmosphere. Luminescence spectral intensities were normalized to Ru concentration.

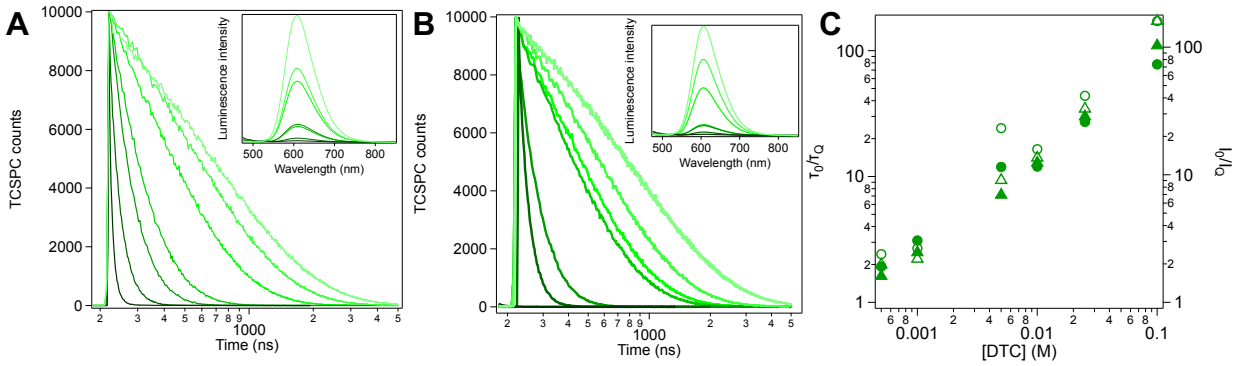

Figure S21. Stern-Volmer quenching analysis of S78C-RuZnAz vs. S78C-RuZnAz-[**1**] with DTC. (**A**) TCSPC decay traces of S78C-RuZnAz and (*inset*) corresponding luminescence spectra. (**B**) TCSPC traces of S78C-RuZnAz-[**1**] and (*inset*) corresponding luminescence spectra. (**C**) Stern-Volmer plot of S78C-RuZnAz (closed markers) vs. S78C-RuZnAz-[**1**] (open markers) using both I_0/I_Q (circles) and τ_0/τ_Q (triangles) ratios for analysis. Samples contained 5 μM RuZnAz in 750 mM phosphate/12.5 mM CHES buffer, pH 7.25, in the presence of 0, 0.5, 1, 5, 10, 25, and 100 mM DTC. All experiments performed under a CO_2 atmosphere. Luminescence spectral intensities were normalized to Ru concentration.

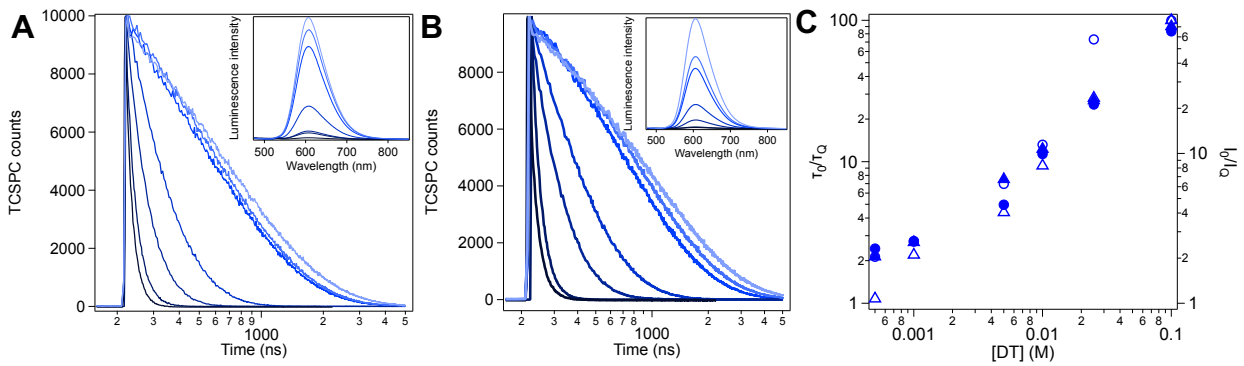

Figure S22. Stern-Volmer quenching analysis of S78C-RuZnAz vs. S78C-RuZnAz-[**1**] with DT. (**A**) TCSPC decay traces of S78C-RuZnAz and (*inset*) corresponding luminescence spectra. (**B**) TCSPC traces of S78C-RuZnAz-[**1**] and (*inset*) corresponding luminescence spectra. (**C**) Stern-Volmer plot of S78C-RuZnAz (closed markers) vs. S78C-RuZnAz-[**1**] (open markers) using both I_0/I_Q (circles) and τ_0/τ_Q (triangles) ratios for analysis. Samples contained 5 μM RuZnAz in 750 mM phosphate/12.5 mM CHES buffer, pH 7.25, in the presence of 0, 0.5, 1, 5, 10, 25, and 100 mM DT. All experiments performed under a CO_2 atmosphere. Luminescence spectral intensities were normalized to Ru concentration.

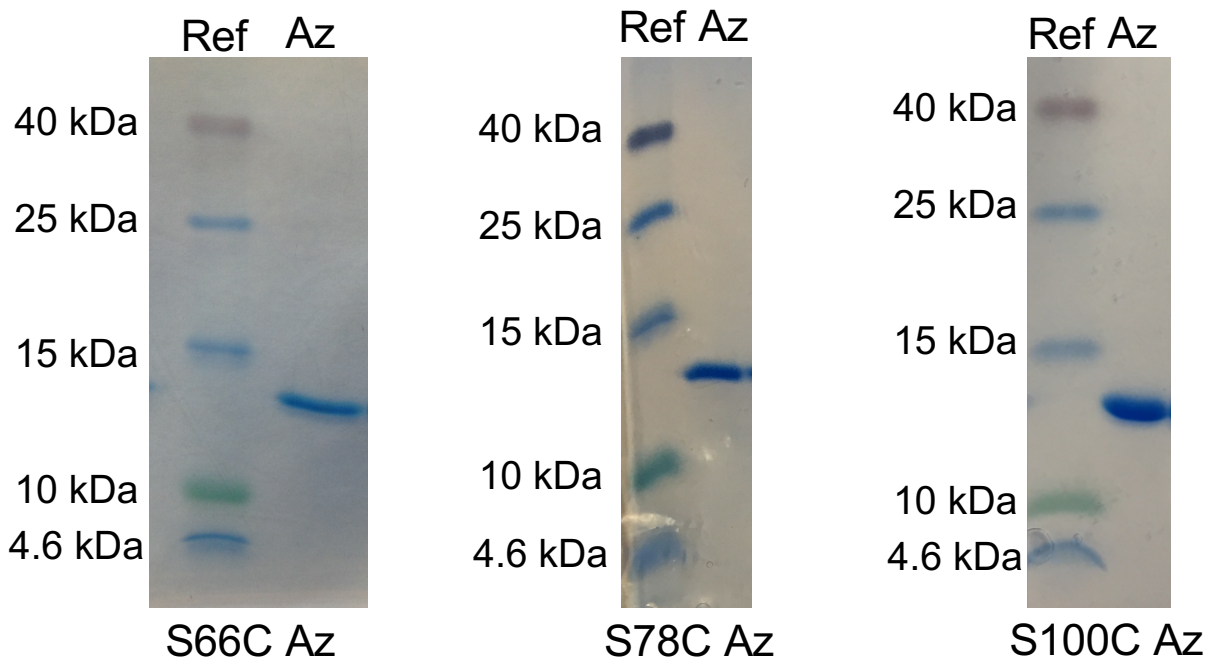

Figure S23. 15% SDS-PAGE of Az mutants. Left-hand lane in each panel shows the reference lane (Spectra Multicolor Low Range Protein Ladder, Thermo Scientific); right-hand lane shows the purified Az variant.

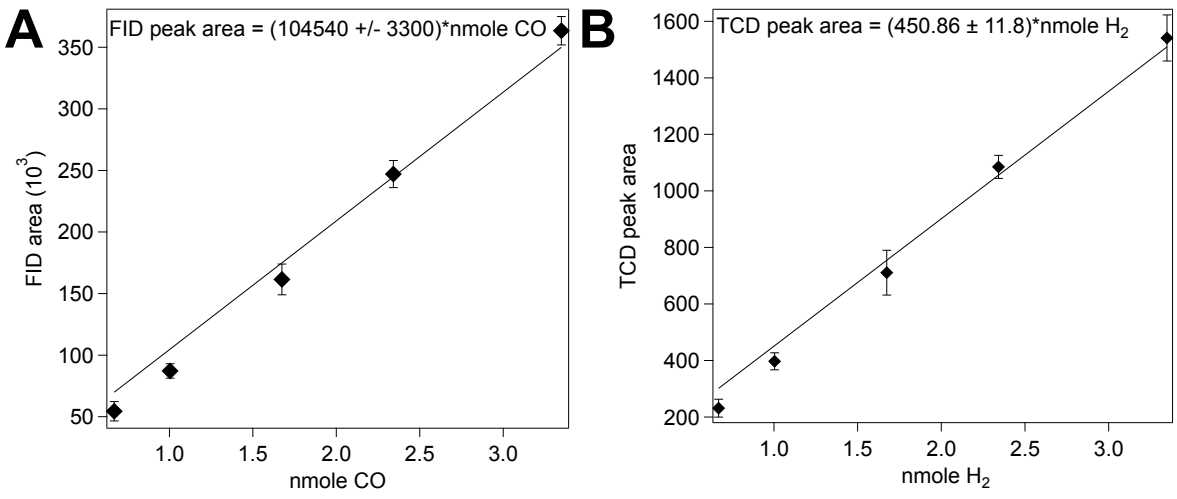

Figure S24. GC calibration curve used for (**A**) CO detection by the FID detector and (**B**) H_2 detection by the TCD detector.

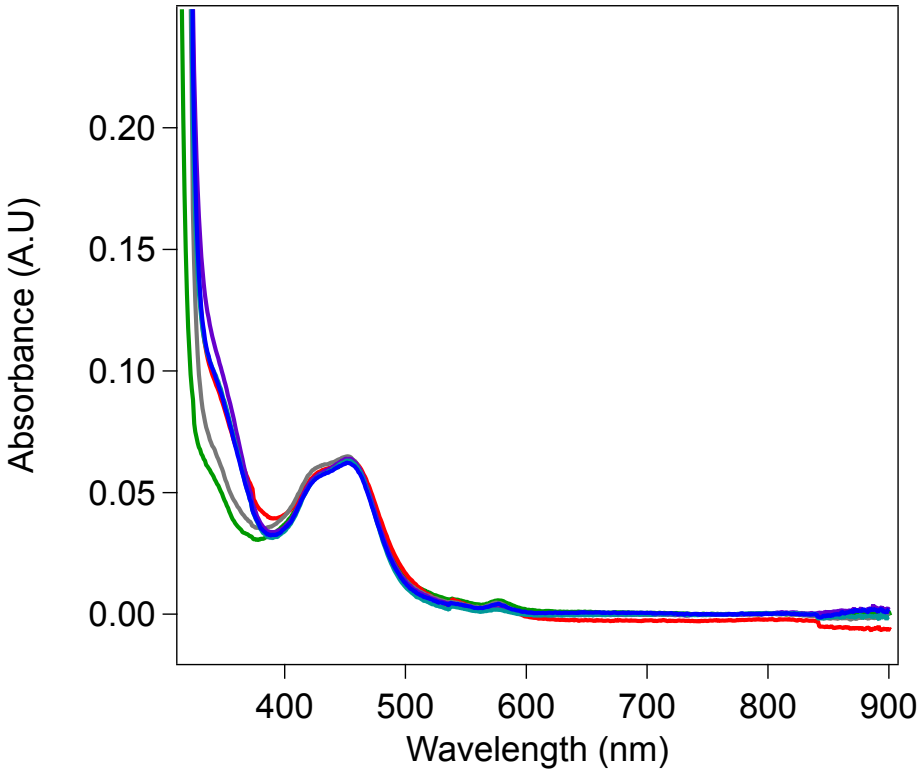

Figure S25. UV-vis spectra of S66C-RuCuAz-[**1**] (gray), S78C-RuCuAz-[**1**] (purple), S100C—RuCuAz-[**1**] (teal), S66C-RuZnAz-[**1**] (red), S78C-RuZnAz-[**1**] (green), and S100C-RuZnAz-[**1**] (blue) under catalytic conditions. Samples contained 5 μM RuMAz-[**1**] in 750 mM phosphate/12.5 mM CHES buffer, pH 7.25, with 100 mM ascorbate under a CO_2 atmosphere. Absorbance due to ascorbate obscures all signals beyond ~300 nm.

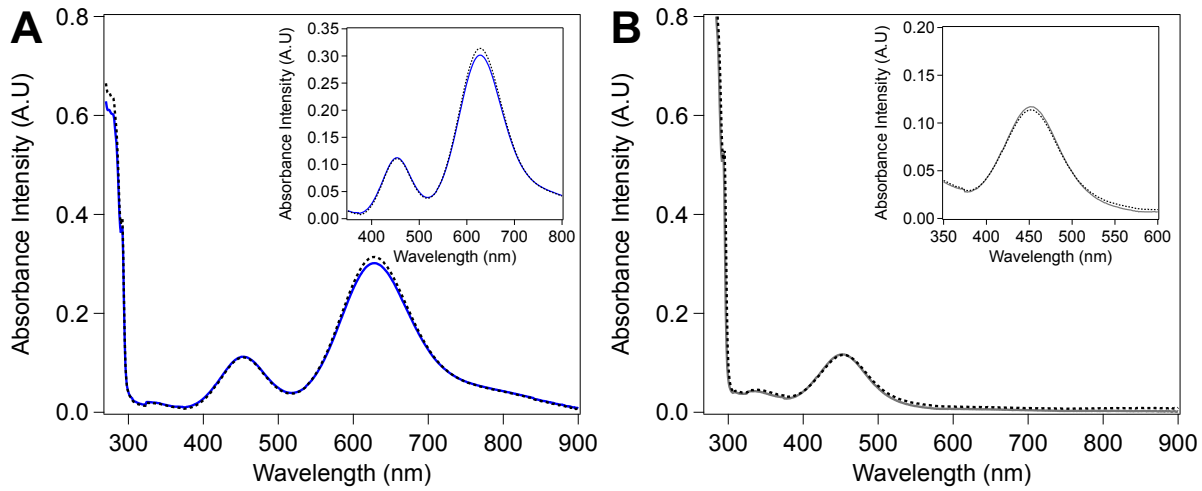

Figure S26. UV-vis spectra of (**A**) WT $Cu^{II}Az$ and (**B**) WT $Zn^{II}Az$ in the presence of excess [**1**]. Samples contained 50 μM $M^{II}Az$ + 2.5 mM [**1**] in 750 mM phosphate/12.5 mM CHES buffer, pH 7.25. Spectra prior to (solid lines) and following (dotted lines) 4 hours of incubation are shown. Free [**1**] absorbs at 450 nm with $\varepsilon \approx 40\ M^{-1}\ cm^{-1}$.

Supplemental References

1 A. C. Manesis and H. S. Shafaat, *Inorg. Chem.*, 2015, **54**, 7959–7967.
2 C. R. Schneider and H. S. Shafaat, *Chem Commun.*, 2016, **52**, 9889–9892.
3 B. C. Larson, J. R. Pomponio, H. S. Shafaat, R. H. Kim, B. S. Leigh, M. J. Tauber and J. E. Kim, *J. Phys. Chem. B*, 2015, **119**, 9438–9449.
4 H. S. Shafaat, B. S. Leigh, M. J. Tauber and J. E. Kim, *J. Am. Chem. Soc.*, 2010, **132**, 9030–9039.
5 H. Wei, J. Yin and E. Wang, *Anal. Chem.*, 2008, **80**, 5635–5639.
6 S. Dwaraknath, N.-H. Tran, T. Dao, A. Colbert, S. Mullen, A. Nguyen, A. Cortez and L. Cheruzel, *J. Inorg. Biochem.*, 2014, **136**, 154–160.
7 B. Bosnich, C. K. Poon and M. L. Tobe, *Inorg. Chem.*, 1965, **4**, 1102–1108.
8 D. J. Sommer, M. D. Vaughn and G. Ghirlanda, *Chem Commun.*, 2014, **50**, 15852–15855.
9 P. T. Maugeri, J. J. Griese, R. M. Branca, E. K. Miller, Z. R. Smith, J. Eirich, M. Högbom and H. S. Shafaat, *J. Am. Chem. Soc.*, 2018, **140**, 1471-1480.
10 X. Ma and H. Tian, *Photochemistry and Photophysics. Concepts, Research, Applications;* Wiley-VCH Verlag: Weinheim, Germany, 2014.
11 S. L. Murov, I. Carmichael and G. L. Hug, *Handbook of Photochemistry, Second Edition*, CRC Press, 1993.
12 A. Juris, V. Balzani, F. Barigelletti, S. Campagna, P. Belser and A. von Zelewsky, *Coord. Chem. Rev.*, 1988, **84**, 85–277.